International Symposium
On Turbulence and Shear Flow
Phenomena (TSFP-8)
August 28 - 30, 2013 Poitiers, France

DYNAMIC MODE DECOMPOSITION OF PIV MEASUREMENTS FOR CYLINDER WAKE FLOW IN TURBULENT REGIME

Gilles Tissot, Laurent Cordier, Nicolas Benard, Bernd R. Noack
PPRIME Institute, CEAT, 43 route de l'aérodrome, 86000 Poitiers, France
Gilles.Tissot@univ-poitiers.fr

ABSTRACT

Dynamic Mode Decomposition (DMD) is a new post-processing technique that can extract from snapshots dynamic informations relevant for the flow. Without explicit knowledge of the dynamical operator, the DMD algorithm determines eigenvalues and eigenvectors of an approximate linear model. DMD can be viewed as a non linear generalization of global stability classically used for a linearized system. This algorithm can be used to determine the eigen-elements of the Koopman operator, an infinite dimensional linear operator associated with the nonlinear system. The ability of DMD to extract dynamically relevant features of the flow has been tested on an experimental PIV dataset of a turbulent cylinder wake flow.

Keywords : cylinder wake, dynamic mode decomposition, reduced-order model

INTRODUCTION

For a turbulent flow, the number of active degrees of freedom is so important that a preliminary step of *model reduction* is necessary for having a chance to understand the flow physics or to derive a control strategy. The general objective of model reduction is to extract, from physical insights or mathematical tools, the building blocks which play a dominant role in terms of modelling. In the case of flow control, this question of educing physically-relevant structures is even more difficult since by definition the flow dynamics will be fully modified by the introduction of the control. Reduced-order modelling is then more an art than a science and finding the appropriate basis for representing the flow in a low-dimensional space is strongly related to a given objective. Indeed, it is somewhat different for a flow to understand the instability mechanisms, to educe the coherent structures mainly responsible for the energy or to represent the non-linear dynamics.

In this communication, we are focusing on a procedure recently introduced by Schmid (2010) called Dynamic Mode Decomposition (DMD). This algorithm was proposed as a method that is able to extract dynamically relevant flow features from time-resolved experimental (Schmid, 2009; Schmid *et al.*, 2009, 2010) or numerical (Tu *et al.*, 2011; Rowley *et al.*, 2009*a*) data. Following Schmid (2010), the DMD modes generalize the global stability modes since it is not necessary with this method to have an explicit knowledge of the dynamical operator to evaluate frequencies and growth rates associated to each DMD mode. Moreover, we will see that DMD can be used to determine the eigenvalues and eigenvectors of the Koopman operator (Rowley *et al.*, 2009*b*), an infinite-dimensional linear operator associated with the full nonlinear system.

In section 1, Dynamic Mode Decomposition is first discussed in terms of model reduction. Then, the DMD algorithm is described in broad outline as in Schmid (2010). Section 2 will present practical considerations necessary to implement the DMD algorithm presented in section 1. Finally, in section 3, the DMD will be demonstrated on experimental data corresponding to a PIV dataset of a cylinder wake flow at Reynolds number 40000.

1 DYNAMIC MODE DECOMPOSITION

1.1 DMD and model reduction

Mathematically, model reduction can be described as a projection method where the dynamical process of interest is projected on an appropriate subspace of small size. For physical reasons or practical considerations, the spatio-temporal solution $\boldsymbol{u}(\boldsymbol{x},t)$ where $\boldsymbol{x}$ corresponds to the spatial coordinate and t denotes time, is often searched as a separated representation

$$\boldsymbol{u}(\boldsymbol{x},t) = \sum_{i=1}^{N_a} \theta_i(t)\Xi_i(\boldsymbol{x}). \qquad (1)$$

For a dynamical process of given complexity, the number N_a of modes in the expansion (1) depends exclusively on the choice of the spatial functions Ξ_i. With an *a posteriori* model reduction technique, the spatial modes are first determined (section 1.2) and then used (section 2.2) to determine by projection the temporal coefficients θ_i. When the dynamics of the system is linear, the eigenvectors of the global stability problem, the so-called *global modes*, are often considered to derive a reduced-order model. This model is known to accurately describe the linearized dynamics of the system. When the dynamics becomes fully non linear, in the turbulent regime for instance, then the Proper Orthogonal Decomposition or POD (Cordier & Bergmann, 2008) is the most well-known and used reduction approach. POD is widely used since it extracts from a sequence of data an orthonormal basis which captures optimally the flow energy. Unfortunately, energy level is not necessarily the correct criterion in terms of dynamical modelling and deriving a dynamical system based on POD modes leads sometimes to

irrelevant models. Here, the DMD algorithm will be presented as a method useful to describe the dynamical behaviour of the system in the linear and non linear regime.

1.2 General description of the DMD algorithm

The data is represented in the form of a snapshot sequence, given by a matrix V_1^N defined as

$$V_1^N = (\boldsymbol{v}_1, \ldots, \boldsymbol{v}_N) \in \mathbb{R}^{N_x \times N} \tag{2}$$

where $\boldsymbol{v}_i$ is the i^{th} snapshot. In the previous definition, the subscript 1 denotes the first member of the sequence, while the superscript N denotes the last entry in the sequence. Moreover, in this temporal framework of DMD, we assume that the snapshots are separated by a constant sampling time Δt.

The DMD algorithm is built on two main assumptions. The first hypothesis is that there exists a linear operator $\mathscr{A}$ to step forward in time the snapshots. Since V_1^N is finite-dimensional, this operator is written as a matrix $A \in \mathbb{R}^{N_x \times N_x}$ such that

$$\boldsymbol{v}_{i+1} = A\boldsymbol{v}_i, \quad \text{for} \quad i = 1, \cdots, N-1. \tag{3}$$

It follows that the subspace spanned by the data set

$$V_1^N = \left(\boldsymbol{v}_1, A\boldsymbol{v}_1, \ldots, A^{N-1}\boldsymbol{v}_1\right) \tag{4}$$

corresponds to the N^{th} Krylov subspace $\mathscr{K}_N(A, \boldsymbol{v}_1)$ generated by A from $\boldsymbol{v}_1$ (Ipsen & Meyer, 1998).

The goal of DMD is to determine the eigenvalues and eigenvectors of A but without first determining A. As such, DMD can be interpreted as an extension of the classical Arnoldi algorithm used to determine eigen-elements of large size problems (Bagheri, 2010). In the Arnoldi algorithm, the knowledge of A is exploited to determine an orthonormal basis for the projection subspace of the Rayleigh-Ritz procedure. In the DMD algorithm, the orthonormal basis of the projection subspace is determined with a "matrix-free" point of view by considering that only snapshots obtained from a time-stepper are available. The matrix A is no longer necessary but the price will be an ill-conditioning of the procedure (see section 2.1).

When the number of snapshots of the sequence V_1^N increased, it is reasonable to assume that, beyond a given number of snapshots, $\boldsymbol{v}_i$ becomes linearly dependent. The second hypothesis is then to consider that the N^{th} iterate writes as a linear combination of the previous iterates *i.e.*

$$\begin{aligned} \boldsymbol{v}_N &= c_1\boldsymbol{v}_1 + c_2\boldsymbol{v}_2 + \cdots + c_{N-1}\boldsymbol{v}_{N-1} + \boldsymbol{r} \\ &= V_1^{N-1}\boldsymbol{c} + \boldsymbol{r} \end{aligned} \tag{5}$$

where $\boldsymbol{c}^T = (c_1, c_2, \cdots, c_{N-1})^T$ and $\boldsymbol{r} \in \mathbb{R}^{N_x}$ is the residual vector. Following Ruhe (1984), we may write

$$AV_1^{N-1} = V_2^N = V_1^{N-1}C + \boldsymbol{r}\boldsymbol{e}_{N-1}^T \tag{6}$$

where $\boldsymbol{e}_i$ is the i^{th} Euclidean unitary vector of length $(N-1)$ and C a Companion matrix defined as

$$C = \begin{pmatrix} 0 & 0 & \ldots & 0 & c_1 \\ 1 & 0 & \ldots & 0 & c_2 \\ 0 & 1 & \ldots & 0 & c_3 \\ \vdots & \vdots & \vdots & \vdots & \vdots \\ 0 & 0 & \ldots & 1 & c_{N-1} \end{pmatrix} \in \mathbb{R}^{(N-1)\times(N-1)}. \tag{7}$$

The Companion matrix C is uniquely defined by the coefficients c_i. The eigen-elements of C are then only dependent on c_i. Indeed, as soon as these coefficients are known, the characteristic polynomial of the transpose of C can be calculated:

$$P_{C^T}(\lambda) = \lambda^{N-1} - \sum_{i=1}^{N-1} c_i \lambda^{i-1}. \tag{8}$$

Moreover, since the eigenvalues of a matrix and its transpose are the same then the eigenvalues and eigenvectors of the Companion matrix C can be determined. We will see in section 2.2 the different ways for evaluating the coefficients c_i.

Let $(\boldsymbol{y}_i, \lambda_i)$ be the i^{th} eigen-elements of C, it can be easily proved using (6) that $\left(\boldsymbol{\Phi}_i = V_1^{N-1}\boldsymbol{y}_i, \lambda_i\right)$ are approximated eigen-elements of A, the so-called Ritz eigenvectors and eigenvalues. The value of the residual $\boldsymbol{r}$ is a good measure of the approximation *i.e.* of the success of the DMD algorithm. We will see in section 1.4 that these Ritz eigenvalues can be used to determine the frequency and the growth rate of the linear process.

A few remarks are appropriate at this point. There is no normalization step in the algorithm. Then, the Ritz eigenvectors are known except for a scaling factor. We will see in section 1.3 that this scaling factor will be retrieved by exploiting some properties of the Companion matrix. Moreover, contrary to the POD modes, the Ritz eigenvectors are not orthonormal. The determination of the temporal coefficients $\theta_i(t)$ will thus require an extra effort. Different possible strategies will be presented in section 2.3.

1.3 Eigen-elements of the Companion matrix

Provided that the eigenvalues $\{\lambda_i\}_{i=1}^{N-1}$ of the Companion matrix are distinct, it can be demonstrated (Rowley *et al.*, 2009*b*) that C can be diagonalized as $C = T^{-1}\Lambda T$ where T is the Vandermonde matrix defined by

$$T = \begin{pmatrix} 1 & \lambda_1 & \lambda_1^2 & \cdots & \lambda_1^{N-2} \\ 1 & \lambda_2 & \lambda_2^2 & \cdots & \lambda_2^{N-2} \\ \vdots & \vdots & \vdots & \vdots & \vdots \\ 1 & \lambda_{N-1} & \lambda_{N-1}^2 & \cdots & \lambda_{N-1}^{N-2} \end{pmatrix} \tag{9}$$

and $\Lambda = \text{diag}(\lambda_1, \cdots, \lambda_{N-1})$. We then have an analytical expression for the eigenvectors of C that is based only on the eigenvalues λ_i. The matrix $\widetilde{\Phi} = (\widetilde{\boldsymbol{\Phi}}_1, \cdots, \widetilde{\boldsymbol{\Phi}}_{N-1})$ of the Ritz eigenvectors is given by

$$\widetilde{\Phi} = V_1^{N-1}T^{-1} \in \mathbb{R}^{N_x \times (N-1)}. \tag{10}$$

Since T is invertible, (10) writes $V_1^{N-1} = \widetilde{\Phi} T$ or

$$\boldsymbol{v}_k = \sum_{i=1}^{N-1} \lambda_i^{k-1} \widetilde{\boldsymbol{\Phi}}_i \quad k = 1, \cdots, N-1. \tag{11}$$

Moreover, we can deduce from $V_2^N = V_1^{N-1} C + \boldsymbol{r} \boldsymbol{e}_{N-1}^T$ that

$$\boldsymbol{v}_N = \sum_{i=1}^{N-1} \lambda_i^{N-1} \widetilde{\boldsymbol{\Phi}}_i + \boldsymbol{r} \text{ with } \boldsymbol{r} \perp \text{span}(\boldsymbol{v}_1, \cdots, \boldsymbol{v}_{N-1}). \tag{12}$$

In the DMD algorithm, the eigenvectors $\widetilde{\boldsymbol{\Phi}}_i$ are called the DMD modes and the eigenvalues λ_i, the DMD eigenvalues.

1.4 Link with linear systems

A discretized version of the expansion (1) written at any time instant $k = 1, \cdots, N-1$ for the Ritz eigenvectors reads:

$$\boldsymbol{v}_k = \sum_{i=1}^{N-1} \boldsymbol{\Phi}_i \theta_i(k). \tag{13}$$

Using the first hypothesis (3), it can be immediately shown that

$$\begin{aligned} \boldsymbol{v}_{k+1} &= A\boldsymbol{v}_k = \sum_{i=1}^{N-1} A\boldsymbol{\Phi}_i \theta_i(k) = \sum_{i=1}^{N-1} \lambda_i \boldsymbol{\Phi}_i \theta_i(k) \\ &= A^k \boldsymbol{v}_1 = \sum_{i=1}^{N-1} \lambda_i^k \boldsymbol{\Phi}_i \theta_i(1). \end{aligned} \tag{14}$$

The DMD eigenvalues $\{\lambda_i\}_{i=1}^{N-1}$ thus dictate the growth rate and frequency of each mode. Since in stability we are interested in the eigenvalues of the time-continuous matrix associated to the time-discrete matrix A of the linear map, it can be proved (Bagheri, 2010) that the growth rate σ_i and frequency ω_i are given by

$$\sigma_i = \frac{\ln(|\lambda_i|)}{\Delta t} \quad \text{and} \quad \omega_i = \frac{\arg(\lambda_i)}{\Delta t}.$$

We can deduce from this discussion that the most striking features between POD and DMD modes is that while a given DMD mode contains only a single frequency component, a POD mode contains in general a continuous spectrum. As a closing remark, we see that based on the Ritz eigenvalues and eigenvectors, (14) can be employed to reconstruct the snapshots as soon as $\theta_i(1)$ is known. This expression will be used in section 3 to reconstruct the data. Finally, by comparing (14) with (11), we can conclude that $\widetilde{\boldsymbol{\Phi}}_i = \boldsymbol{\Phi}_i \theta_i(1)$. $\theta_i(1)$ is then the scaling factor that links the eigenvectors of the Companion matrix C to the Ritz eigenvectors obtained by the DMD algorithm presented in section 1.2.

2 PRACTICAL CONSIDERATIONS

In this section, we will discuss practical considerations necessary to apply the DMD algorithm as described in section 1.2. Since DMD is a data-based analysis method, the characteristics of the dataset (value of time step, number of snapshots) are crucial. These points are discussed in section 2.1. Once the dataset is chosen, the next ingredient is the numerical method used to determine the coefficients of the Companion matrix C. Different approaches will be presented in section 2.2. Finally, when the DMD modes are known, we would like to reconstruct the original temporal dynamics. For this, we need to determine the temporal coefficients $\theta_i(t)$. Different oblique projection methods are discussed in section 2.3.

2.1 Choice of the dataset

In the original framework introduced by Schmid (2010), DMD extracts dynamic modes which can be interpreted as a generalization of global stability modes when the flow is linearized and as a linear tangent approximation of the underlying dynamics for non linear flow. Whatever the flow regime considered, an important parameter is then the value of the constant time step Δt between successive snapshots. Obviously, in order for the DMD to extract pertinent flow processes, the flow must be sampled at a sufficiently high frequency. However, if this sampling frequency is too high then the snapshots will have a tendency to be correlated in time and the DMD modes will not be unique following Chen *et al.* (2012). The interpretation of Ritz eigenvalues and eigenvectors in terms of global stability is then subjected to an *a priori* good knowledge of the physical process under study in order to choose correctly the value of Δt.

The choice of the number N of snapshots contained in V_1^N is also a matter of discussion. Indeed, for the DMD to be unique, the first $N-1$ snapshots have to be linearly independent and the N^{th} snapshot should be written as a linear combination of the previous ones (second DMD hypothesis, Eq. (5)). However, in most of the physical data, the end of the linear independence is not so sudden. One way of checking linear independence of the snapshots is to use the Gram-Schmidt process. In an intermediate step of this process, a sequence of vectors defined as

$$\boldsymbol{b}_j = \boldsymbol{v}_j - \sum_{l=1}^{j-1} (\boldsymbol{v}_j, \boldsymbol{b}_l) \boldsymbol{b}_l \quad \text{for} \quad j = 1, \cdots, N$$

is produced where $(\cdot,\cdot)$ stands for the Hermitian inner product *i.e.* $(\boldsymbol{w}_1, \boldsymbol{w}_2) = \boldsymbol{w}_1^H \boldsymbol{w}_2$. The variation with j of the ratio $\|\boldsymbol{b}_j\|/\|\boldsymbol{v}_j\|$ where $\|\boldsymbol{b}_j\|^2 = (\boldsymbol{b}_j, \boldsymbol{b}_j)$ gives a good indication of the loss of linear independence when new snapshots are added. Figure 1 corresponds to the case of the experimental data used in section 3. The decrease of $\|\boldsymbol{b}_j\|/\|\boldsymbol{v}_j\|$ is rather slow indicating that the choice of the number of snapshots to be processed by DMD is not obvious. As a consequence, the DMD algorithm will be probably ill-conditioned and the DMD modes may not be physically relevant. One way of checking the DMD procedure is to *a posteriori* determine the value of the residual $\boldsymbol{r}$ defined in (5).

2.2 Coefficients of Companion matrix

So far, the DMD algorithm was given (section 1.2) but without describing how the coefficients c_i of the Companion matrix C were found. The objective of this section is to present different methods that can be considered. It is possible in practice to:

1. Apply a QR factorization to V_1^{N-1} *i.e.*

$$\boldsymbol{v}_N = V_1^{N-1} \boldsymbol{c} = QR\boldsymbol{c} \quad \text{or} \quad \boldsymbol{c} = R^{-1} Q^H \boldsymbol{v}_N \tag{15}$$

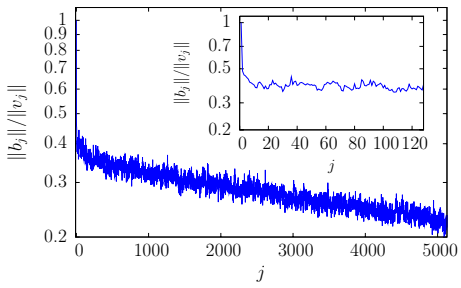

Figure 1. Variation of the normalized residual of the Gram-Schmidt process with the index of the snapshot.

where Q^H is the hermitian conjugate of Q.

2. Perform a SVD of V_1^{N-1} *i.e.*

$$\begin{aligned} &\boldsymbol{v}_N = V_1^{N-1}\boldsymbol{c} = U_{\mathrm{SVD}}\Sigma_{\mathrm{SVD}}V_{\mathrm{SVD}}^H\boldsymbol{c} \quad \text{or} \\ &\boldsymbol{c} = V_{\mathrm{SVD}}\Sigma_{\mathrm{SVD}}^{-1}U_{\mathrm{SVD}}^H\boldsymbol{v}_N. \end{aligned} \tag{16}$$

3. Take the inner product of (5) with $\boldsymbol{v}_j$ for $j = 1,\cdots,N-1$. We obtain: $\left(\boldsymbol{v}_N,\boldsymbol{v}_j\right) = \sum_{i=1}^{N-1}\left(\boldsymbol{v}_i,\boldsymbol{v}_j\right)c_j$.
If we now introduce the correlation matrix $K_{ij} = \left(\boldsymbol{v}_i,\boldsymbol{v}_j\right)$ and the vector $\boldsymbol{w} = \left(K_{N1},\cdots,K_{NN-1}\right)^T$, we arrive to the linear system of equations

$$\boldsymbol{c} = K^{-1}\boldsymbol{w}. \tag{17}$$

These three methods require a matrix inversion that can be done only if the snapshots $\{\boldsymbol{v}_i\}_{i=1}^{N-1}$ are linearly independent. So here we find with a numerical point of view the results of uniqueness presented in Chen *et al.* (2012).

2.3 Determination of the coefficients $\theta_i(k)$

Equations (13) and (14) can be used to reconstruct the temporal dynamics of the snapshots from the Ritz eigenvalues and eigenvectors. However, the temporal coefficients $\theta_i(k)$ first need to be known at all the time instants $k = 1,\cdots,N$ or at the minimum at the first instant $k = 1$. Indeed, by identifying (13) and (14), it can be deduced immediately that

$$\theta_i(k+1) = \lambda_i^k\theta_i(1), \quad \text{for} \quad k = 1,\cdots,N-1. \tag{18}$$

Since the Ritz eigenfunctions are not orthonormal, two oblique projection methods are here proposed to determine $\theta_i(k)$.

2.3.1 Gramian matrix

A first idea is to use the Gramian matrix G of $\Phi = (\boldsymbol{\Phi}_1,\cdots,\boldsymbol{\Phi}_{N-1})$ whose entries are given by $G_{ij} = (\boldsymbol{\Phi}_i,\boldsymbol{\Phi}_j)$. Taking the inner product of (13) with $\boldsymbol{\Phi}_i$, $i = 1,\cdots,N-1$, we obtain the linear system of equations

$$G\,\boldsymbol{\theta}_k = \boldsymbol{z}_k \quad \text{for} \quad k = 1,\cdots,N$$

where $\boldsymbol{\theta}_k = (\theta_1(k),\cdots,\theta_{N-1}(k))^T$ and $\boldsymbol{z}_k = ((\boldsymbol{\Phi}_1,\boldsymbol{v}_k),\cdots,(\boldsymbol{\Phi}_{N-1},\boldsymbol{v}_k))^T$. This relation can be written in matrix form as

$$\theta = G^{-1}\Phi^H V_1^N, \tag{19}$$

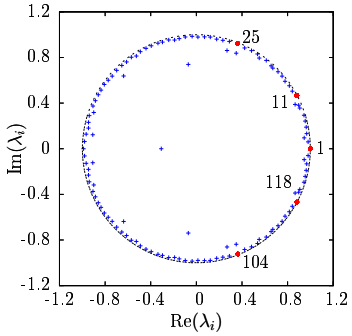

Figure 2. Empirical Ritz values λ_i.

where θ is the matrix that contains the vectors $\boldsymbol{\theta}_k$. For using (19), the matrix G must be well conditioned.

2.3.2 Adjoint basis

Another solution is to search for adjoint modes $\boldsymbol{\Psi}_j$ of $\boldsymbol{\Phi}_i$. Indeed, if the adjoint modes are know then it is straightforward to determine the coefficients $\theta_j(k)$ as

$$\theta_j(k) = \sum_{i=1}^{N-1}\underbrace{\left(\boldsymbol{\Psi}_j,\boldsymbol{\Phi}_i\right)}_{\delta_{ij}}\theta_i(k) = \left(\boldsymbol{\Psi}_j,\boldsymbol{v}_k\right). \tag{20}$$

By definition, $\boldsymbol{\Psi}_i$ is solution of the adjoint eigenvalue problem

$$A^H\boldsymbol{\Psi}_i = \bar{\lambda}_i\boldsymbol{\Psi}_i. \tag{21}$$

It can be easily proved that $\left(\boldsymbol{z}_i = \left(V_1^{N-1}\right)^H\boldsymbol{\Psi}_i,\bar{\lambda}_i\right)$ are approximated eigen-elements of C^H. Since V_1^{N-1} is in general a non-square matrix, we can use the SVD decomposition of V_1^{N-1} (Moore-Penrose pseudoinverse) for finding that

$$\boldsymbol{\Psi}_i = U_{\mathrm{SVD}}\Sigma_{\mathrm{SVD}}^{-1}V_{\mathrm{SVD}}^H\boldsymbol{z}_i. \tag{22}$$

3 RESULTS

The DMD algorithm has been performed on data obtained by 2D-2C PIV measurements for a turbulent cylinder wake (Benard *et al.*, 2010) corresponding to a sub-critical flow regime ($Re_D = DU_\infty/\nu_{\mathrm{kin}} = 40000$ where $D = 40\,\mathrm{mm}$ is the cylinder diameter and $U_\infty = 15.6\ m.s^{-1}$ is the free-stream velocity). The database contains $N_s = 5130$ snapshots taken at a sampling frequency $f_s = 1\,\mathrm{kHz}$ over approximatively 400 periods of vortex shedding. Following the discussions in section 2.1, the DMD is applied on 128 snapshots (see Fig. 1) without subtracting the mean. Here, the coefficients $\boldsymbol{c}$ were calculated with (17) by inverting the correlation matrix K.

Figure 2 shows that nearly all the Ritz values are on the unit circle indicating that the snapshots lie on or near an attracting set. The growth rate of each DMD mode σ_i is plotted versus its frequency ω_i in Fig. 3. The spectrum appears symmetric with respect to the imaginary axis $\omega_i = 0$,

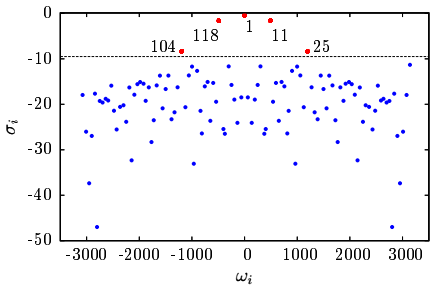

Figure 3. Time-continuous DMD spectrum of the cylinder wake flow.

which is a consequence of processing real-valued data. Indeed, in that particular case, the eigenvalues and associated eigenvectors are real or complex conjugate. At this point, the Ritz eigenvectors are available for the design of a reduced-order model. However, it remains to be decided which of the modes should be included in the reduction basis. One criterion that should be assessed is based on the damping rate of the DMD and employs the argument that modes with large decay rates are dynamically less relevant than modes that are only weakly damped. Figure 3 suggests that the mean flow and the two first pairs of modes should be sufficient to obtain a good description of the dynamics. The most amplified mode (mode 1) corresponds to the mean flow. The streamwise Φ_1^u and spanwise Φ_1^v components of $\mathbf{\Phi}_1$ are plotted in Fig. 6. The complex conjugates modes 11 and 118 oscillate at $St = 0.2$ (see Fig. 4) which is precisely the fundamental shedding frequency of the wake flow. Figure 6 contains also the streamwise and spanwise components of $\mathbf{\Phi}_{11}$ and $\mathbf{\Phi}_{25}$, respectively. The modes 118 and 104 are not represented for symmetry reasons.

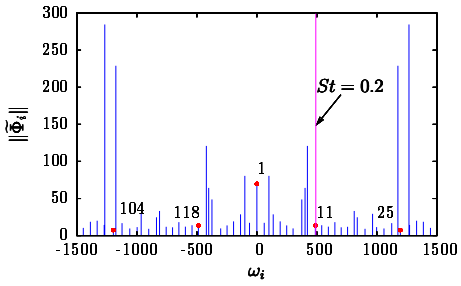

Figure 4. Magnitudes of the DMD modes at each frequency ω_i.

Figure 4 represents the amplitude of the DMD modes. Their amplitudes are not a criterion in itself of the dynamic relevance of these modes since even a mode with a very large amplitude can be strongly damped. For instance, the mode 11 corresponding dynamically to the vortex shedding ($St = 0.2$) has relatively low amplitude compared to other modes.

Concerning the temporal coefficients $\theta_i(k)$ of the Ritz eigenvectors, they are represented in Fig. 5 for the three dominant modes: 1, 11, and 25. For symmetry reasons, the temporal coefficients θ_{118} and θ_{104} are again not plotted. The three methods proposed in section 2.3 to determine the temporal coefficients, respectively with the Gramian matrix (19), the adjoint modes (20) and the multiplication of the Ritz eigenvalues by $\theta_i(1)$ (see Eq. (18)) have been compared and give exactly the same results. The amplitude of the mean flow is approximatively constant over time. The oscillatory behaviour of the vortex shedding mode 11 is well captured and the mode 25 is clearly damped. Knowing $\theta_i(1)$, it was *a posteriori* checked that $\widetilde{\mathbf{\Phi}}_i = \mathbf{\Phi}_i \theta_i(1)$.

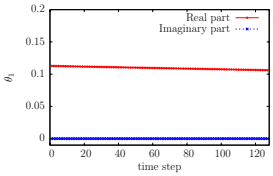

(a) $\theta_1(k)$.

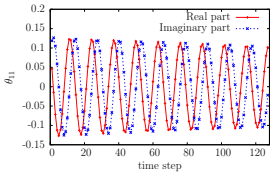

(b) $\theta_{11}(k)$.

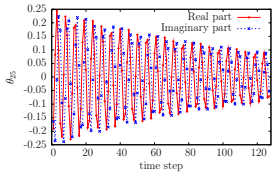

(c) $\theta_{25}(k)$.

Figure 5. Temporal coefficients of the DMD modes.

In order to assess the possibility of deriving an accurate reduced-order model based on some DMD modes, different reconstructions of the snapshot $\boldsymbol{v}_5$ have been performed (see Fig. 7). Figures 7(c) and 7(d) correspond to the reconstruction of the streamwise u and spanwise v components of $\boldsymbol{v}_5$ using all the DMD modes. Compared to the original fields represented in Figs. 7(a) and 7(b), respectively, a very good agreement is obtained. The error in L^2 norm is about 0.07%. If the number of DMD modes kept in the reconstruction is reduced, the tendency is to describe increasingly large space scales. When the modes 1, 11, 118, 25 and 104 are used for the reconstruction (Figs. 7(e) and 7(f)), the L^2 error is 42.5%. When the modes in the reconstruction are still reduced to 1, 11 and 118 (Figs. 7(g) and 7(h)), the L^2 error decreases up to 40.5%. Due to the non orthogonality of the DMD modes, the L^2 error is not monotonic with the number of modes as it is the case by definition for the POD modes. These reduced-order approximations may be on some circumstances (flow control for instance) sufficient good approximations of the physical phenomena.

4 CONCLUSION

DMD is a method that is able to extract dynamic information from empirical data obtained either numerically or in experiments. Without explicit knowledge of the underlying dynamical operator, it determines growth rates, frequencies and spatial structures of an approximate linear model. These modes can be viewed as a generalization of global stability modes obtained for a linearized system. The DMD algorithm was presented in details. Lastly, it was shown that a reduced-order model based on the three most unstable pairs of DMD modes can reproduce qualitatively well the original dynamics.

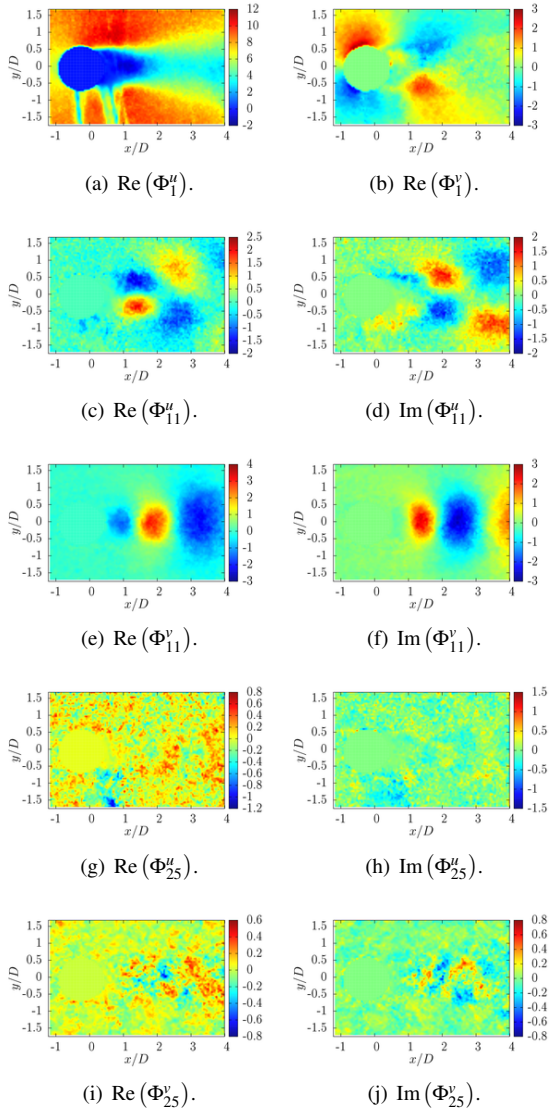

(a) Re (Φ_1^u). (b) Re (Φ_1^v).

(c) Re (Φ_{11}^u). (d) Im (Φ_{11}^u).

(e) Re (Φ_{11}^v). (f) Im (Φ_{11}^v).

(g) Re (Φ_{25}^u). (h) Im (Φ_{25}^u).

(i) Re (Φ_{25}^v). (j) Im (Φ_{25}^v).

Figure 6. DMD modes 1, 11 et 25.

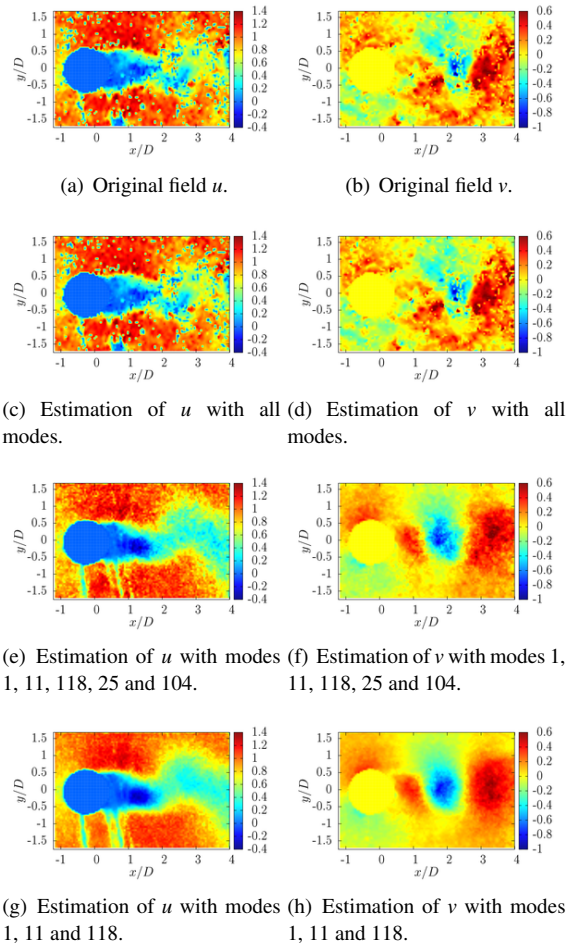

(a) Original field u. (b) Original field v.

(c) Estimation of u with all modes. (d) Estimation of v with all modes.

(e) Estimation of u with modes 1, 11, 118, 25 and 104. (f) Estimation of v with modes 1, 11, 118, 25 and 104.

(g) Estimation of u with modes 1, 11 and 118. (h) Estimation of v with modes 1, 11 and 118.

Figure 7. Reconstruction of the streamwise u and spanwise v components of the snapshot $\boldsymbol{v}_5$.

References

Bagheri, S. 2010 Analysis and control of transitional shear flows using global modes. PhD thesis, Department of Mechanics Royal Institute of Technology SE-100 44 Stockholm, Sweden.

Benard, N., Debien, A., David, L. & Moreau, E. 2010 Analyse par PIV rapide du sillage d'un cylindre manipulé par actionneurs plasmas. In *Congrès Francophone de Techniques Laser*. Vandoeuvre-lès-Nancy 14-17 septembre.

Chen, K. K., Tu, J. H. & Rowley, C. W. 2012 Variants of Dynamic Mode decomposition: Boundary Condition, Koopman, and Fourier Analyses. *Journal of Nonlinear Science* **22** (6), 887–915.

Cordier, L. & Bergmann, M. 2008 Proper Orthogonal Decomposition: an overview. In *Lecture series 2002-04, 2003-03 and 2008-01 on post-processing of experimental and numerical data*. Von Kármán Institute for Fluid Dynamics.

Ipsen, I.C.F. & Meyer, C.D. 1998 The idea behind Krylov methods. *American Mathematical Monthly* **105** (10), 889–899.

Rowley, C.W., Mezić, I., Bagheri, S., Schlatter, P. & Henningson, D.S. 2009*a* Reduced-order models for flow control: balanced models and Koopman modes. In *Seventh IUTAM Symposium on Laminar-Turbulent Transition*, pp. 43–50. Springer.

Rowley, C.W., Mezić, I., Bagheri, S., Schlatter, P. & Henningson, D.S. 2009*b* Spectral analysis of nonlinear flows. *Journal of Fluid Mechanics* **641**, 115–127.

Ruhe, A. 1984 Rational Krylov Sequence Methods for Eigenvalue Computation. *Lin. Alg. Appl.* **58**, 391–405.

Schmid, P.J. 2009 Dynamic Mode Decomposition of experimental data. In *8th International Symposium on Particle Image Velocimetry*.

Schmid, P.J., Li, L., Juniper, MP & Pust, O. 2010 Applications of the Dynamic Mode Decomposition. *Theoretical and Computational Fluid Dynamics* pp. 1–11.

Schmid, P.J., Meyer, K.E. & Pust, O. 2009 Dynamic Mode Decomposition and Proper Orthogonal Decomposition of flow in a lid-driven cylindrical cavity. In *8th International Symposium on Particle Image Velocimetry*.

Schmid, P. J. 2010 Dynamic Mode Decomposition of numerical and experimental data. *Journal of Fluid Mechanics* **656**, 5–28.

Tu, J.H., Rowley, C.W., Aram, E. & Mittal, R. 2011 Koopman spectral analysis of separated flow over a finite-thickness flat plate with elliptical leading edge. *49th AIAA Aerospace Sciences Meeting including the New Horizons Forum and Aerospace Exposition 4-7 January 2011, Orlando, Florida* .